First Quasi-snwoflake Divertor Experiment on EAST

B.J. Xiao[1,2], G. Calabrò[3], Y. Guo[1], Z.P. Luo[1], R. Albanese[4], R. Ambrosino[4], L. Barbato[4], F. Crisanti[3], G. De Tommasi[4], E. Giovannozzi[3], S. Mastrostefano[4], A. Pironti[4], V. Pericoli Ridolfini[4], G. Ramogida[3], A.A. Tuccillo[3], F. Villone[4], B. Viola[3], R. Zagórski[5]

[1]*Institute of Plasma Physics, Chinese Academy of Sciences, Hefei, 230031, China*

[2]*School of Nuclear Science and Technology, University of Science and Technology of China, Hefei, 230026, China*

[3]*ENEA Unità Tecnica Fusione, C.R. Frascati, Via E. Fermi 45, 00044 Frascati, Roma, Italy*

[4]*CREATE, Università di Napoli Federico II, Università di Cassino and Università di Napoli Parthenope, Via Claudio 19, 80125 Napoli, Italy*

[5]*Institute of Plasma Physics and Laser Microfusion, Warsaw, Poland*

Abstract: Heat and particle loads on the plasma-facing components are among the most challenging points to be solved for ITER and a reactor design. Alternative magnetic configuration, such as the X-divertor, Super X-divertor and Snowflake divertor may enable tokamak operation at lower peak heat load than a standard Single Null divertor. This paper reports on the modelling of the variations of the second null point present in the advanced magnetic divertor, here so-called quasi-Snowflake configuration, and first experiments performed on the EAST tokamak in 2014.

1. Introduction

Handling fusion power and particle exhaust, reducing heat loads below a limit on plasma-facing components, especially on divertor plates, are one of the critical issues for the long-pulse or steady-state operation ITER and future fusion reactor. Plasma detachment from a divertor target is one of the most attractive methods for handling the exhaust power and fusion ash, sparing the divertor targets from unacceptable localized power loads [1]. Another approach to handling the heat exhaust power is to use alternative magnetic configurations, such as the snowflake divertor (SF) [2] and the single-legged X-divertor [3]. The single-legged X divertor places the second X-point near the plate, casuing flared field lines there, which spreads the heat over a larger area and increases the line connection length. The SF configuration is characterized by a second-order null (X-point) in the poloidal magnetic field (B_p), where both B_p itself and its spatial derivatives vanish ($B_p = 0, \nabla B_p = 0$). This splits the separatrix near the null into six segments: two of them enclose the confined plasma and four lead to the machine wall (the divertor legs) [4]. The poloidal cross-section of the obtained magnetic flux surfaces with a hexagonal null-point has the appearance of a snowflake. Theoretical studies indicate that the SF magnetic geometry may led to both higher power losses during scrape-off layer (SOL) transport and an increased plasma wetted area of the wall [5,6]. The former results from an increase in the connection length and the divertor volume, the latter from an increase in flux expansion and SOL width. The SF was estabilished on TCV[7], NSTX [8] and DIIID [9].

Exact SF configuration has several problems (for instance are intrinsically

unstable) and for this reason the first experiments performed on the Experimental Advanced Superconducting Tokamak (EAST) and discussed in this paper, are mainly devoted to the study of the role of the reciprocal position of the two x-points characterizing the so-called quasi-SF (QSF) configuration. Each of them in its vicinity behaves as a first-order null, with the magnetic field growing linearly with the distance from the null, but the coefficient in this linear dependence 'knows' of the presence of the second null. This coefficient depends linearly on the distance between the nulls, as discussed in SF's theory [10] and, in a close vicinity of each null, does not depend on the direction.

As shown in Fig. 1, EAST is constructed to be up-down symmetric, with the following main parameters [11]: major radius R = 1.8 m, minor radius a = 0.45 m, toroidal field B_T up to 3.5 T, and plasma current I_p up to 1 MA for highly elongated plasma with elongation κ = 1.9. It can be operated in quite flexible plasma shapes with an elongation factor κ = 1.5-2.0 and triangularity δ = 0.3-0.6 for double null (DN) or SN divertor configurations. EAST is equipped with 14 superconducting poloidal field coils (PFCs) for ohmic heating, ohmic current drive, shaping and position control [12]. It should be noted that PFCs 7 and 9 are connected in series as are PFCs 8 and 10. Thus, there are in total 12 independent PF power supplies (maximum current I_{PF} = 14.5kA). EAST also has in-vessel active feedback coils (IC coils) for fast control of the plasma vertical instability; they consist of two 2-turn coils symmetrically located in the upper and lower part of the vessel and connected in anti-series in order to provide an horizontal field. Unlike DIII-D and NSTX, EAST does not have dedicated divertor coils which could be used to shape the local flux distribution within the divertor region. It should be noted that in EAST, due to the location of PF coils and target plates, as will be discussed in the next section, the secondary x-point could be moved around from the primary one to form a magnetic configuration that features the SF+/- (characterized by a contracting geometry near the plate) or an X divertor (X-d) configuration (characterized by a flaring geometry near the plate). In the rest of the paper, we shall refer to the configurations and related experiments with a two-null divertor geometry as quasi-SF (QSF) scenarios, indicating for each configuration the features of contracting or flaring geometry.

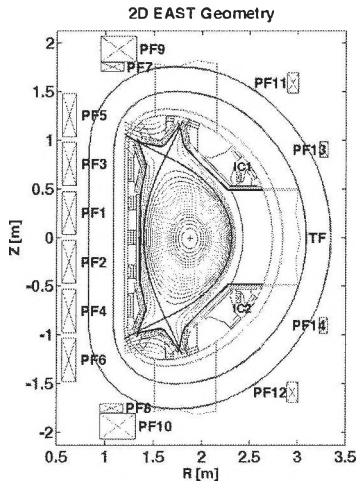

Figure 1. Tow-dimensional EAST geometry schematic view.

2. EAST QSF equilibria modeling and optimization

QSF equilibria have been designed and optimized by means of CREATE-NL code [13], in combination with EFIT [14] and FIXFRESS [15] codes. The tokamak simulation code (TSC) [16], a numerical model of the axisymmetric tokamak plasma and the associated control systems, has been then used to model the EAST QSF full plasma time evolution scenario. The procedure proposed for the design and optimization of QSF equilibrium using the CREATE-NL code exploits the linearized relation between the plasma-wall gaps and the PF currents, as discussed in reference [17]. It is composed of two steps:

1) the first step allows to have a first cut of the QSF equilibrium starting from a standard single null plasma configuration: a new equilibrium with a second null point within a limited distance from SN x-point is obtained, forcing the plasma boundary to be almost unchanged, apart from the region in the vicinity of the null point;

2) the second step refines the plasma shape and possibly reduces the PF coil currents while fulfilling the machine technological constraints.

Here, QSF equilibria are identified as modifications of experimental reference EAST SN discharge #43362 (I_P ~ 400kA, B_T = 1.8T, internal plasma inductance l_i ~ 1.4, poloidal beta β_p ~ 0.1) with the following constraints to be verified:

a) PF coil currents I_k far enough from their limits: $I_{min} + \Delta I \leq I_k \leq I_{max} - \Delta I$, with $\Delta I = 0.1 \max\{|I_{min}|, |I_{max}|\}$;

b) vertical instability growth rate not much larger than reference SN configuration;

c) strike points on vertical targets;

d) at least 40 mm clearance (gap) between plasma boundary and first wall.

The objectives of the QSF design and optimization procedure consists in the definition of a set of QSF equilibria, at low (0.1) and high β_p (0.45) with the secondary x-point close or far from the vessel structures maximizing the plasma

current. The optimized QSF configurations obtained with CREATE-NL and then verified by EFIT and FIXFREE code are summarized in Table I. The simulated QSF and experimental reference SN equilibria at low β_p are shown in Figure 2.

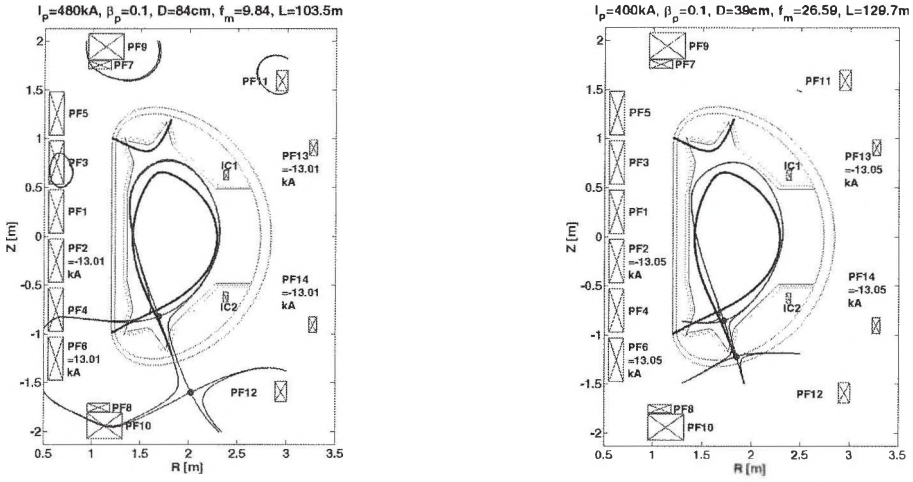

Figure 2. Plasma boundary of optimized QSF (blue solid line) and reference SN equilibria (black solid line), at low β_p, calculated by CREATE-NL code. Also the x-point separation D, the connection length L, the polodal magnetic flux expansion f_m in outer SP region and maximum obtained PF currents are reported for QSF equilibria. For the SN configuration: L=95m, f_m=2.1.

For the QSF configurations with I_P=400 kA the secondary x-point is located on the vessel (on the inner shell at low beta, on the outer shell location for a high beta plasma, not shown here), see figure 2.

However, the secondary x-point point may be brought inside the vessel at the price of a slightly lower plasma current or a higher plasma elongation and/or a futher optmization of the coil corrents. Finally, the "close nulls" QSF equilibria present higher flux expansion on the divertor plates. The high β_p configurations (not shown here) are slightly more demanding in terms of PF currents.

Table I. EAST optimized QSF configurations by CREATE-NL code

	QSF low β_p 400kA "close nulls"	QSF high β_p 400kA "close nulls"	QSF low β_p 480kA "far nulls"	QSF high β_p 480kA "far nulls"	Reference SN 43362
I_P [kA]	400	400	480	480	388
β_p	0.1	0.45	0.1	0.45	0.1
l_i	1.4	1.4	1.4	1.4	1.26
IPF1 [A]	2560	3789	3366	6897	-196
IPF2 [A]	-13050	-13051	-13016	-13027	-203
IPF3 [A]	9407	9513	6635	4319	222
IPF4 [A]	2707	2028	2050	306	-1432
IPF5 [A]	-9398	-12706	-7363	-10229	2158
IPF6 [A]	13050	13051	13016	13027	3956
IPF7_9 [A]	1198	2649	2222	4020	5233
IPF8_10 [A]	-970	-742	218	566	5282
IPF11 [A]	5322	4368	4033	2769	-6055
IPF12 [A]	7145	6779	5557	5255	-5981

IPF13 [A]	-13050	-13051	-13016	-13027	-192
IPF14 [A]	-13050	-13051	-13016	-13027	-622
max(abs(currents)) [A]	13050	13051	13016	13027	6055
x-points separation D (only for QSF cases)	39	45	84	92	-
κ	1.73	1.72	1.71	1.71	1.65
Volume [m^3]	12.21	12.59	12.28	12.76	11.02
Flux Expansion f_m	26.59	22.29	9.84	11.09	2.09
Connection length L (m)	129.74	126.23	103.50	101.47	94.93
Growth rate lower bound [s^{-1}]	186	161	148	120	88
Growth rate upper bound [s^{-1}]	474	339	341	241	195
Growth rate with 3D model [s^{-1}]	454	312	258	198	120
Stability margin with 2D model	0.46	0.52	0.55	0.66	0.86

3 Experimental results

First QSF experiments have been performed on EAST in 2014, after nearly 20-month-long upgrading break. In these experiments the simplest form of plasma current and position (i.e. plasma centroid) control has been used, the so-called RZIP control [18]. The control parameters are regulated by adjusting the current in PF coils. The requested PF coil current is composed of the sum of feed-forward (FF) and feedback (FB) components. The PFC currents discussed in Section 2 have been used as FF component target in RZIP control for QSF experiments (here only "far nulls" case). Magnetic and plasma characteristics of QSF have been studied in discharges with I_P = 0.25MA and B_T = 1.8T, κ ~ 1.9, q_{95} ~ 8, ohmic and with 0.4MW of NBI heating. It should be noted that the plasma current in this first QSF experiments has been purposely kept low for safety reasons. Figure 3 shows the experimental magnetic equilibria at different time, reconstructed with EFIT using standard magnetic constraints for ohmic discharge #47660. In EAST, as previously discussed, the secondary x-point could be moved around and configurations could vary from a SF to X-d divertor configuration.

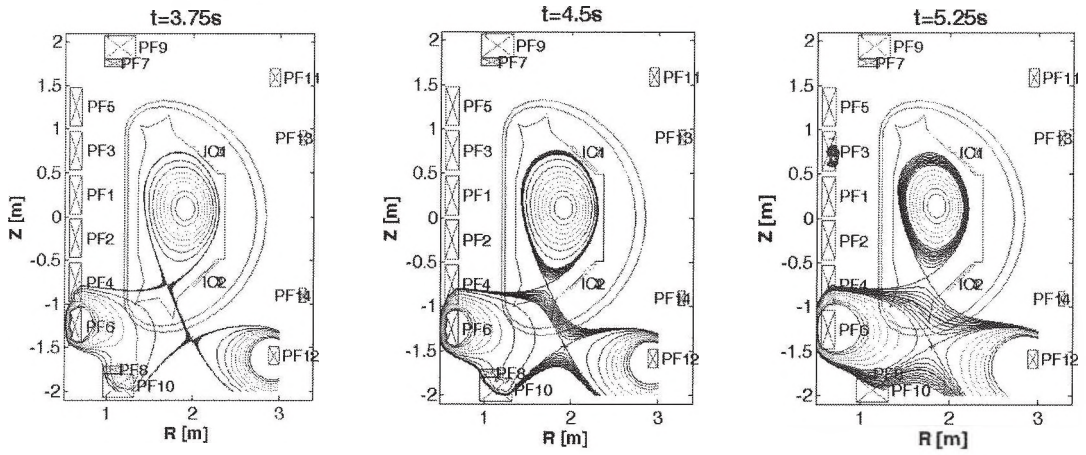

Figure 3. Sequence of EFIT equilibria for ohmic QSF discharge #47660 at 3.75, 4.5 and 5.25s.

A simple comparison between QSF and lower single null (LSN) are carried on in

experiment. Shot 48971 is QSF experiment with NBI injected at 4.00, while shot 47038 is LSN configuration with LHW injection. The plasma quantities are similar after 4.5 sec, shown as figure 4. Diverter probes give the spatial-temporal profile of ion saturation current density jsat for these two shots, shown as figure 5. jsat is stable for LSN discharge. For QSF discharge, jsat at the outer target significantly decreases after 4.5 sec when the QSF configuration is formed. It indicates QSF could reduce the heat flux on the divertor. In figure 6. the EFIT reconstructed equilibria for QSF #48971 (at t=4.5s, with β_p = 0.76 and l_i = 1.28) and SN #47038 (at t=4.5s, with β_p = 0.58 and l_i = 1.56) discharges are shown. Experimental magnetic geometry properties for both configurations are compared in Table II.

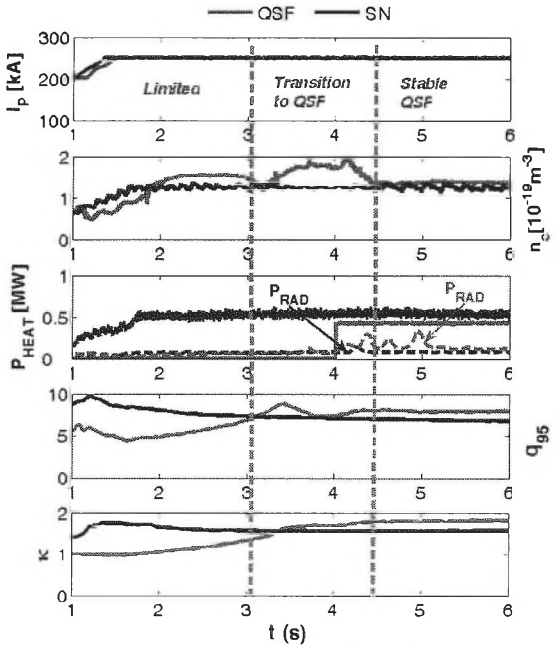

Figure 4. Time evolution of main plasma quantities for LSN (#47038, black line) and QSF (#48971, red line)

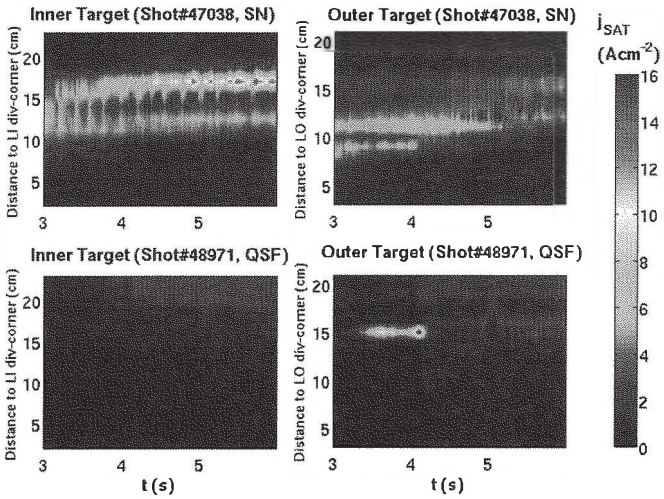

Figure 5. Spatio-temporal profiles of ion saturation current density j_{SAT} for SN (#47038) and QSF discharge (#48971). Once QSF configuration becomes stable, the peak of j_{SAT} is observed to drastically drop indicating a possible heat flux reduction.

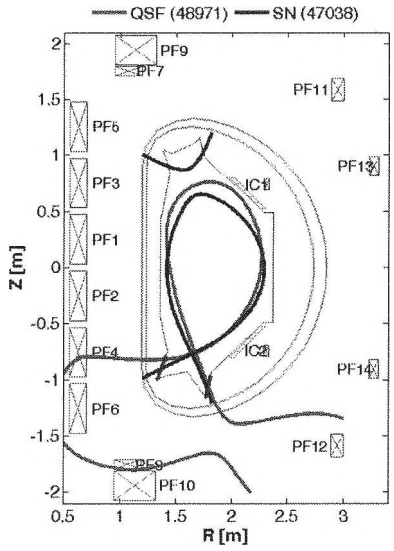

Figure 6. Schematic 2D view of EAST with SN #47039 at t=4.5s (black solid line) and QSF (red solid line) at t=4.5s plasma boundaries. The x-point separation D is = 79cm for the QSF discharge.

Table II: Main magnetic geometry for SN and QSF configurations, assuming SOL width at midplane of 2mm

	QSF, #48971 at t=4.5s	**SN, #47038 at t=4.5s**
SOL Volume [m^3]	0.389	0.260
Connection Length [m]	189.91	144.38
Magnetic flux expansion at outer SP $f_{m,out}$	8.22	2.01
Magnetic field angle at outer SP α_{out} [deg]	0.33	1.22
Magnetic flux expansion at inner SP $f_{m,in}$	4.71	2.34
Magnetic field angle at inner SP α_{in} [deg]	0.90	1.29

These results confirm the predictions discussed in the previous sections: the presence of a secondary null-point in QSF reduces B_p/B_{tot} in the divertor separatrix region, where B_{tot} is total magnetic field, and this increases the connection length by ~30% and the flux expansion in the outer SP region by a factor ~4. This obtained QSF configuration shows a value PF6 = 8.3kA as the maximum current during the discharge evolution, well below the limit. The experimental connection length is higher than the predictive one, discussed in section 2, of a factor ~1.5 for both QSF and SN, as expected due to the fact that the experimental I_P is ~45% lower than the simulated one.

4 Conclusions

It has been experimentally demonstrated that the possibility of creating and controlling the two-null divertor QSF configuration on EAST. In the present preliminary experiments, the presence of a secondary X-point increases the connection length by ~30% and the flux expansion in the outer SP region by a factor

~4, confirming the predictions of the optimization study set up by CREATE-NL tools in combination with EFIT and FIXFREE codes. It has been observed that in L-mode discharge the peak of ion saturation current density drops once the QSF configuration becomes stable compared to SN case, which could indicate a heat flux reduction. These first experiments also indicate that the plasma current could be increased by a further optimization of the configuration and that it is possible to play around with the reciprocal distance of the two X-points in order to change the topological features of the configuration. In the coming EAST experiments the already upgrade of ISOFLUX control system will allow to control the exact position of secondary X-point. This will permit to the increase the additional heating power and to easily vary some of the features of the topological configuration.

References

[1] A. R. Raffray, et al., *Fusion Eng. Des.*, 39-41, 323-348, 1998.
[2] D. D. Ryutov, et al., *Phys. Plasmas*, 14, 064502, 2007
[3] M. Kotschenreuther, et al., *Phys. Plasmas*, 20, 102507, 2013
[4] W. A. Vijvers, et al., *Nucl. Fusion*, 54, 023009, 2014
[5] D. D. Ryutov, et al., *Phys. Plasma*, 15, 092501, 2008
[6] D. D. Ryutov, et al., *Phys. Scr.*, 89, 88002, 2014
[7] F. Piras, et al., *Plasma Phys. Control. Fusion*, 51, 055009, 2009
[8] V. A. Soukhanovskii, et al., *J. Nucl. Mater.*, 415, S365-8, 2011
[9] S. Allen, et al., *Proc. 24th Int. Conf. on Fusion Energy (San Diego, CA, 8-13 October 2012)*, 2012
[10] D. D. Ryutov, et al., *Plasma Phys. Control. Fusion*, 52, 105001, 2010
[11] Y. X. WAN, et al., *Overview progress and future plan of EAST Project Proc. 21th Int. Conf. on Fusion Energy 2006 (Chengdu, China 2006) (Vienna: IAEA)* CD-ROM file OV/1-1 and www-naweb.iaea.org/napc/physics/fec/fec2006/html/index.htm

[12] B.J. XIAO, et al., *Fusion Eng. Des.*, **83,** 181, 2008

[13] M. Mattei, et al., CREATE-NL+: a robust control-oriented free boundary dynamic plasma equilibrium solver *28th Symp. on Fusion Technology (San Sebastian, Spain 2014)* P1.036
[14] L. L. Lao, et al., *Nucl. Fusion*, 25, 1611, 1985
[15] F. Alladio, and F. Crisanti, *Nucl. Fusion*, 26, 1143, 1986
[16] Y. Guo, et al., *Plasma Phys. Control. Fusion*, 54, 085022, 2012
[17] R. Albanese, et al., *Plasma Phys. Control. Fusion*, 56, 035008, 2014
[18] B. J. Xiao, et al., *Fusion Eng. Des.*, 87, 1887, 2012